INTERNATIONAL JOURNAL OF CLIMATOLOGY
Int. J. Climatol. **25**: 1405–1419 (2005)
Published online in Wiley InterScience (www.interscience.wiley.com). DOI: 10.1002/joc.1198

HEAT STORAGE AND ANTHROPOGENIC HEAT FLUX IN RELATION TO THE ENERGY BALANCE OF A CENTRAL EUROPEAN CITY CENTRE

B. OFFERLE,[a,b,*] C. S. B. GRIMMOND[a] and K. FORTUNIAK[c]

[a] *Atmospheric Sciences Program, Department of Geography, Indiana University, 701 E. Kirkwood, Bloomington, IN 47405, USA*
[b] *Göteborg University, Göteborg, Sweden*
[c] *University of Łódź, Łódź, Poland*

Received 13 February 2004
Revised 16 March 2005
Accepted 16 March 2005

ABSTRACT

The role of net heat storage ΔQ_S and anthropogenic heat Q_F are considered in the surface energy balance for a downtown area in Łódź, Poland, for a 2 year period. Eddy covariance measurements provide estimates of the turbulent heat fluxes and radiometric measurements of the net all-wave radiation. A method to determine ΔQ_S based on representative surface temperature sampling is employed and compared with results from two other models. Results show that ΔQ_S is an important flux on the scale of hours to days and that it can be more than 10 W m^{-2}, on average, for periods of a week or more. By incorporating ΔQ_S estimates over hourly intervals, Q_F was then determined as the residual of the energy balance. Using the approach, Q_F averaged 32 W m^{-2} from October to March (60% of available energy), and -3 W m^{-2} from June to August. The physically unrealistic negative values for the summer period may suggest underestimation of turbulent fluxes, but no causal factor was identified. Although energy balance closure was close to 100% throughout the year, there was weaker agreement in the winter. This is attributed to errors in estimates of ΔQ_S and variation in Q_F. Results highlight the need for future investigations of the urban surface energy balance to incorporate more complete measurements and estimates of ΔQ_S. Copyright © 2005 Royal Meteorological Society.

KEY WORDS: urban energy balance; storage heat flux; anthropogenic heat flux

1. INTRODUCTION

Although a number of studies have now been published on the surface energy balances (SEBs) of urban areas (e.g. Grimmond and Oke, 2002; Spronken-Smith, 2002), most of these studies rely on direct observations of just three of the SEB fluxes (i.e. the net all-wave radiation Q^*, the turbulent latent heat Q_E, and sensible heat Q_H fluxes), with few direct measurements of the heat storage ΔQ_S or estimates of the anthropogenic heat Q_F flux terms (Nemitz *et al*., 2002). These prior investigations have indicated that the magnitude of the net change in heat storage ΔQ_S is more significant to the energy balance of urban areas than many other land covers, bare soil or agricultural landscapes (Grimmond and Oke, 1999; Wilson *et al*., 2002) and that this flux is an important determinant of distinct features of urban climates. For example, the magnitude of ΔQ_S slows the response of the surface to changes in radiative and atmospheric forcing, and thus dampens the amplitude of turbulent heat fluxes. Taha (1999) showed that the inclusion of a simple parameterization for heat storage (the objective hysteresis model (OHM) of Grimmond *et al*. (1991)) improved the representation of urban heat island dynamics in a mesoscale model. Others, notably Rotach (1995), Best and Clark (2002), and Grimmond and Oke (2002), have shown that heat released from storage coupled with the increased roughness of cities helps maintain a more neutral atmospheric profile over the urban surface at night.

* Correspondence to: B. Offerle, Atmospheric Sciences Program, Department of Geography, Indiana University, 701 E. Kirkwood, Bloomington, IN 47405, USA; e-mail: bofferle@indiana.edu

In urban settings the anthropogenic heat flux varies in both time and space. In cities, or parts thereof with intensive industrial or commercial activity, or where there is significant winter heating or summer air conditioning, this term may also be a significant component of the energy balance (Oke, 1987; Klysik, 1996; Ichinose *et al*., 1999). Q_F may be estimated from energy consumption estimates and empirical traffic flow data (Oke, 1987; Grimmond, 1992; Sailor and Lu, 2004). Unfortunately, these data do not all usually match the temporal or spatial scale of the other SEB measurements and may only be compared over longer time frames. Data from energy consumption statistics cited by Oke (1988) suggest that annual average Q_F ranges from 20 to 160 W m^{-2} for large cities, or from 20 to 300% of available energy, making its consideration obligatory for long-term energy balance studies.

The measurement of ΔQ_S at the local scale can be neither simple nor complete (Arnfield and Grimmond, 1998). The number of features (buildings, roads, vegetation, bare soil, etc.) that must be considered and the range of variation among each of these in terms of spatial location and properties is large. Perhaps at best a limited number of measurements may be taken at the building scale and then scaled up to the local scale. The dynamics of heat storage in urban areas have been studied in many local-scale investigations assuming it is well represented as the residual of the measured energy balance (Grimmond and Oke, 1999):

$$\Delta Q_S[\mathrm{W\ m^{-2}}] = Q^* - Q_H - Q_E. \tag{1}$$

This assumes that the contributions of other fluxes not listed in Equation (1) and flux sampling errors are negligible or are otherwise included in ΔQ_S. A more complete energy balance at the interface between the urban surface layer and the atmosphere can be written:

$$Q^* + Q_F = Q_H + Q_E + \Delta Q_S + \Delta Q_A + S \tag{2}$$

where ΔQ_A is the net advected flux and S is all other sources and sinks of energy. Note that the volume is defined such that the flux into the ground is incorporated in ΔQ_S. Most commonly, the turbulent fluxes (Q_H, Q_E) are measured using eddy-covariance (EC) techniques. Over urban surfaces, however, one possible important contribution to S would be rainwater, which absorbs heat from the surface but is channelled out of the system via sewers.

There are a number of uncertainties inherent in this methodology that can lead to an imbalance in Equation (2). These uncertainties and errors have been discussed in detail elsewhere (e.g. Goulden *et al*., 1996; Moncrieff *et al*., 1996; Vickers and Mahrt, 1997; Wilson *et al*., 2002; Su *et al*., 2004). Here, issues of particular importance in the urban environment are highlighted.

Given that the roughness sublayer (RSL) is large for urban areas relative to the inertial sublayer (ISL) (Roth and Oke, 1993; Rotach, 1999), when conducting EC measurements it may be difficult to ensure that instruments are in the ISL. Consequently, the resultant EC measurements may not represent the true spatial average of the surface flux, leading to uncertainties in the measured fluxes. Coupled with this there may be a mismatch between the source areas for the radiative (Q^*) and the turbulent fluxes (Schmid *et al*., 1991; Schmid, 1997). This is not an issue if there is little variability in the source area surface characteristics, and it is not considered a large source of the error in Equation (2) over natural vegetation (Wilson *et al*., 2002). In cities, the height requirements for spatial averaging of Q^* measurements can be greater than for the turbulent fluxes (Offerle *et al*., 2003) and, given the surface heterogeneity of many urban landscapes, differences in surface characteristics between the respective source areas of the two sets of measurements are more likely. That Q^* appears to be spatially conservative over urban areas (Oke, 1997; Offerle *et al*., 2003) may make these possible differences negligible in relation to other errors.

If ΔQ_A and S in Equation (2) are small or unbiased, and the other terms (Q^*, Q_H, Q_E, ΔQ_S) determined directly, then the expected value of the residual term should be an estimate of Q_F, since, from a measurement perspective, it is impossible to remove anthropogenic contributions from the terms in Equation (2). The Q_F term considered here captures only the effects of energy released within the system, which is not necessarily equivalent to energy consumption.

The determination of ΔQ_S is also important for assessing the accuracy of EC measurements. Wilson *et al*. (2002) observed that EC measurements over vegetated surfaces tend to be biased towards zero, hence

underestimating peak daytime heat fluxes and overestimating night-time fluxes for sites that included some independent measure of ΔQ_S. Even without the diurnal bias, over the long term, the ratio of the sum of the turbulent fluxes to available energy, termed the energy balance ratio $\Omega = (Q_H + Q_E)/(Q^* - \Delta Q_S)$, was consistently less than one, with a mean of 0.84 over all site-years (Wilson *et al*., 2002). In urban areas, given the addition of Q_F, the energy balance ratio should be formulated as

$$\Omega = \frac{Q^* + Q_F - \Delta Q_S}{Q_H + Q_E} \tag{3}$$

Even given the difficulties of independently estimating ΔQ_S in urban areas, it may be simpler than estimating Q_F for all measurement source areas at all times, which requires a great deal of information about traffic patterns and energy consumption on short time intervals. Since both terms are of interest, and neither can be neglected, at least one, and preferably both, should be estimated to allow for a complete assessment of the energy balance.

In this paper, attention is focused on the storage and anthropogenic heat fluxes and their significance in the urban surface energy balance using a long-term data set collected in Łódź, Poland (Offerle *et al*., in press).

2. METHODS

2.1. Heat storage estimation on the local scale

The estimation of urban heat storage on the local scale is complicated by the number of elements that need to be measured. For example, a 500 m × 500 m area with an element spacing of 50 m (equivalent to a lot area of 0.25 ha) would contain around 100 buildings. A far simpler approach is to scale up from the building to the local scale based on the average material characteristics of the elements, which include building roof, wall, and internal mass, and road surface, neglecting storage in vegetation but not necessarily the shading effects of the vegetation. This limits the required measurements to a single building, or a few representative buildings, and the surrounding ground surfaces. Assuming that building properties, orientation, shading and wind sheltering effects are consistent over the area in question, the scaled estimate should be representative of the local area. The assumption is better met when the area of interest represents a homogeneous sub-unit of the urban area, such as a neighbourhood with a single land use (e.g. residential) with buildings of approximately the same age. In cases where internal building temperature is rigorously maintained, one could assume no change in internal mass temperature and this component could be neglected.

The problem is still somewhat intractable due to the nature of buildings that incorporate uneven distributions of internal mass, air spaces, and a conglomeration of materials with a range of thermal properties. For example, a roof is likely to be composed of a rough reflective component (crushed stone), to minimize absorbed shortwave radiation and increase sensible heat flux, over a thin impervious layer (asphalt or membrane), over a structural component (wood or concrete), overlying an insulating layer to minimize heat transfer into or out of the building (Meyn, 2000). Direct measurement of all components of heat storage for even a single building is unrealistic.

2.1.1. Element surface temperature method. Overall, it seems more practical and reliable to use a limited number of element surface temperature observations and model the heat transfer through the elements. For convenience this approach is referred to as the element surface temperature method (ESTM). Although heat flux plates can, and have, been used to measure heat flux through building elements (e.g. Nunez and Oke, 1977), it is difficult to implement on a large scale. The primary assumption is that the measured temperatures of a micro-scale unit, which is repeated to create the larger local-scale area, are representative.

To simplify the estimation and scaling of heat storage to rely on the fewest possible measurements, the three-dimensional urban surface was reduced conceptually to a number of one-dimensional elements for building roofs, walls, and internal mass and road, representing the various components of the surface volume (Figure 1). The thickness of each element was determined by the average volume per unit plan area. Note

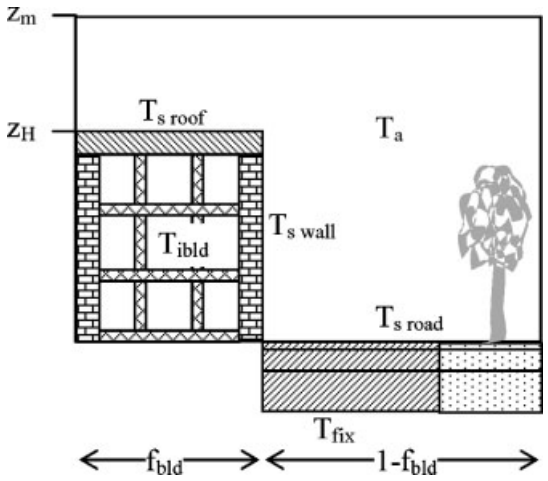

Figure 1. Schematic showing elements used to estimate heat storage flux ΔQ_S. Surface temperatures T_S, internal building temperature T_{ibld}, and air temperature T_a are used to determine ΔQ_S. Storage is calculated for the volume below flux measurement height z_m to the depth of fixed soil temperature T_{fix}. The fraction of surface covered by buildings is denoted f_{bld}. Note that storage in vegetation is neglected and that soil layer properties are averaged into the corresponding road layer

that the element referred to as 'road' incorporates soil heat storage for the vegetation fraction of surface cover as well as the soil beneath the road, although these could also be treated separately if measurements are available. The volume of interest is determined by the height of the flux measurements z_m down to a lower boundary condition of fixed temperature or to a zero flux condition at the base of the volume of interest. This leads to the formulation of the urban volume heat storage flux (W m^{-2}) as

$$\Delta Q_S = \sum_i \frac{\Delta T_i}{\Delta t}(\rho C)_i \Delta x_i \lambda_{pi} \tag{4}$$

where $\Delta T/\Delta t$ is the rate of temperature change over the period, ρC is the volumetric heat capacity, Δx is the element thickness and λ_p is the plan area index. So, $\Delta x \lambda_p$ is simply the total element volume over the plan area, for each element i. Direct conduction from roof to walls and latent heat storage are not considered. Since the average internal element temperature is not directly measured, it can be estimated by combining Fourier's law with the one-dimensional conservation of heat equation:

$$\rho C \frac{\partial T}{\partial t} = -\frac{\partial Q}{\partial x} = -\frac{\partial}{\partial x}\left(-k\frac{\partial T}{\partial x}\right) \tag{5}$$

where Q is the heat flux through the surface and k is the thermal conductivity. This formulation is similar to that employed in urban surface schemes such as Masson (2000) or Kusaka *et al.* (2001).

For the inside surfaces of the roof and walls, and both surfaces for the internal mass (floors, internals walls), the surface temperature T_0 of element i is determined by setting the conductive heat transfer out of (into) the surface equal to the radiative and convective heat losses (gains):

$$k\frac{\Delta T_i}{\Delta x} = \sigma\left(\sum_j \psi_{j\longrightarrow i} T_{0j}^4 - T_{0i}^4\right) - (T_{0i} - T_{bld})C_H \tag{6}$$

where σ is the Stefan–Boltzmann constant, $\psi_{j\to i}$ is the view factor of element j to element i and C_H (W m^{-2} K^{-1}) is the convective exchange coefficient and an emissivity of one is assumed. This allows anthropogenic heat fluxes from building heating, metabolic processes and electric waste heat to be implicitly

incorporated into the model. The convective exchange coefficient was set to 1.2, which is within the range of typical values for natural convection from internal room surfaces (Awbi and Hatton, 1999). The internal view factors were calculated assuming four-storey buildings with a layout of two rows of five rooms of equal size separated by a hallway. The internal building mass (iBLD) dominates the view factors with values of 0.8, 0.9, 0.95 for iBLD $\rightarrow$ iBLD, iBLD $\rightarrow$ wall and iBLD $\rightarrow$ roof respectively.

2.1.2. Measurements and study site. This study was conducted in the downtown of Łódź, Poland (19°27′E, 51°46′N) using SEB flux measurements made over 2001–02. Site characteristics are summarized in Table I. Detailed information about the site, observations, and data processing are given in Offerle *et al*. (in press) and are summarized here.

The instrumentation is mounted 37 m above ground level on a tubular tower (Figure 2). The tower is 20 m tall (top diameter 8 cm) and mounted on the roof of a 17 m building. A complete list of instrumentation and sampling rates is given in Table II. The EC instruments are mounted on booms extending approximately 1 m from the tower, oriented eastward in the direction of the most densely built and extensive fetch. In addition, radiation components (incoming and outgoing shortwave and longwave), air temperature, relative humidity, atmospheric pressure, precipitation, soil heat flux, temperature, and moisture are measured. The soil heat flux Q_G was determined from a heat flux plate embedded 50 mm under the surface, with the flux divergence in the layer above determined by the measured soil temperature change. These instruments were placed near the building's northeast corner, where there is patchy grass cover (Figure 2).

From July to December 2002, infrared measurements of the four wall temperatures of the building hosting the flux measurement tower and the road temperature at the intersection adjacent to the building (Lipowa and Curie streets) were measured. The wall temperature measurements were made approximately three-quarters of the way up the building ($0.75z_H$). The field of view of the infrared thermometer directed to the road included a portion of a deciduous tree canopy. In addition, fast-response thermocouples were used to measure the air column temperature and unshaded roof temperature. As these measurements were not available for the entire time period (2001–02), a linear regression model was used to develop a continuous dataset over the time frame. The regression model determines roof, wall (four-wall mean), and road temperature from the measured radiation components, air temperature and solar zenith angle and their first-order time differences. The root-mean-square error (RMSE) from the data not used for fitting (60% of the data) was below 0.5 °C, and absolute errors did not show a dependence on seasonality.

The reference junction temperature for the datalogger was used as a proxy for the internal building air temperature T_{bld}. Although this measurement includes a slight heating bias from the datalogger, it has a diurnal and seasonal pattern driven by the actual internal air temperature. A greater, spatial inconsistency occurs because the T_{bld} was measured in a top-floor room on the east side of the building, i.e. it heated up more rapidly in the morning than did the building air temperature as a whole. Data averaged over 15 min were used for the storage estimation.

Table I. Characteristics of the Lipowa site (see Offerle *et al*. (in press) for details)

Parameter	
Ellefsen (1994) classification	A2–A4
Theurer (1999) classification	Dense urban development (DUD) or block-edged buildings (BEB)
Oke (2004) urban climate zone classification	2
Mean building height z_H (m)	10.6
Canyon aspect ratio H/W	0.75
Surface fractions (buildings, other impervious, vegetation)	0.3, 0.4, 0.3
Zero-plane displacement z_d (Raupach) (m)	7.4
Roughness length $z_{0,m}$ (Raupach) (m)	1.7
Roughness length $z_{0,m}$ (anemometric) (m)	1.6

Figure 2. Photograph of the measurement site

2.1.3. Model implementation and parameters. The average element depth for building wall and roof thicknesses and internal building mass were estimated assuming all buildings in the 500×500 m^2 grid cell (approximately congruent with the unstable source area of the turbulent flux measurements) of the surface database had the same characteristics as the measured building (Table III). To compute T_i for each element, an explicit finite difference approximation to Equation (5) was used.

To ensure computational stability, the model driving variables were interpolated to 300 s intervals. Three layers were used for roof, walls and internal mass and four layers for the road. As shown in Figure 1, soil and road layer properties were averaged into the single road element. The lower boundary condition for the road element was set equal to the 30 year mean air temperature (Sellers, 1966). Heat storage in the air column was determined from the T_a measurement at 37 m, assuming a neutral temperature profile. There was almost no difference between air column storage calculated with this temperature and that calculated using the temperature profile (eight measurement locations within the volume) over the period 19 July–29 August 2004. Neglected were the latent heat changes in the air column (presumed small on a diurnal basis), heat storage in vegetation, and heat storage in internal building air. The ESTM was run sequentially over 2001–02 twice in succession to minimize initialization errors in temperature distribution.

The main difference between this approach and that employed in urban surface schemes, e.g. the Town Energy Balance (TEB) of Masson (2000), is that the surface temperatures (the top boundary conditions for the elements) are forced rather than diagnosed, such that complex radiation exchanges and turbulent fluxes need not be resolved. Although no measurements of 'actual' local-scale heat storage fluxes are available to validate this approach, the ESTM results are compared with OHM and TEB. TEB was configured using nearly identical landscape parameters, with the exception that four model layers were used for each element. The TEB storage estimate referred to in Section 3.1 includes the ISBA Q_G term for the 30% of land surface covered by vegetation.

Table II. Instrumentation installed at Lipowa. d_{sm} is the distance from sensor to mast. Sample frequency: F is 10 Hz, S15 0.2 Hz and 15 min averaging period; S5 0.2 Hz and 5 min averaging period (source Offerle *et al*. (in press))

Instrument/Model	Manufacturer	d_{sm} (m)	H (m) AGL	Sample frequency
Tower (all at 37 m AGL)				
3-d sonic anemometer/thermometer (K-type) (SN 980 402)	Applied Technologies, Boulder, CO	0.89		F
T-type thermocouple (0.13 mm diameter)	Omega Engineering, Stamford, CT	0.91		F
Krypton hygrometer KH2O (SN 1084)	Campbell Scientific (CSI), Logan, UT	0.99		F
CNR1 net radiometer (SN 000 220)	Kipp & Zonen, Netherlands	0.84		S15
Cup anemometer and vane	RM Young, MI	0.61		S15
MP100H temperature & RH (SN 65 873)	Rotronic, Switzerland	0.37		S15
Roof level				
PTA 427 pressure sensor (SN 465 201)	Vaisala, Finland		16	S15
Surface wetness CS237	CSI		18	S15
Precipitation TE525 (SN 10 697-692)	Texas Electronics, Dallas, TX		18	S15
Ground level				
Soil heat flux HFT3	Radiation Energy Balance Systems		−0.05	S15
Soil temperature TCAV	CSI		−0.03	S15
Volumetric soil moisture CS615	CSI		0 to −0.1	S15
T-type thermocouple (0.13 mm diameter)	Omega		29, 24, 20, 17, 13, 9, 6, 4, roof	S5
Infrared thermometer 4000 A	Everest Interscience, Tucson, AZ		14 (N, E, S, W wall), road	S5

Table III. Properties of layers for heat storage estimation (values based on ASHRAE (1981))

Element	Layer(s)	Material	k (W K^{-1} m^{-1})	ρC (MJ K^{-1} m^{-3})	Δx (m)	λ_p
Roof	1	Asphalt	0.74	1.9	0.03	0.3
	2	Concrete	0.93	1.5	0.12	0.3
	3	Insulation	0.06	0.07	0.05	0.3
External walls	1–3	Concrete and glass	0.95	1.6	0.10	0.8
Internal mass	1–3	Concrete	0.93	1.5	0.05	2.1
Road	1	Asphalt and concrete	0.76	1.5	0.10	0.7
	2	Asphalt	0.74	1.9	0.25	0.7
	3	Sand and gravel	0.63	1.2	1.00	0.7
	4	Sand and gravel	0.63	1.2	3.00	0.7

2.2. Anthropogenic heat flux

The ESTM estimate of ΔQ_S was averaged over the same periods (hourly) as the turbulent fluxes and net radiation, and Q_F was determined as the residual of Equation (2) with advection and other sources or sinks assumed to be zero. Thus, the Q_F term will also incorporate all the errors in measurement and the ΔQ_S model, but only systematic errors will be important over long time scales. It should be noted that this dataset has not been gap-filled for missing data; therefore, the estimates for Q_F form an incomplete time series.

The slope of the linear regression of the sum of the turbulent fluxes on the available energy can be used as an estimate of the degree of energy balance closure (Wilson *et al*., 2002). This assumption is valid for urban areas only if Q_F is incorporated into Equation (3) or is constant over the data. The former is difficult

to implement, as the value for Q_F is hard to estimate over short time intervals, and the latter is not true, since Q_F varies diurnally and with respect to ambient temperature in winter. However, Q_F can be represented by a constant (the time average over the data, $\overline{Q_F}$) with the addition of an error term incorporated into the regression error ε. The slope estimate of closure is then estimated without the need to include Q_F in the available energy and the intercept of the regression is an estimate of $\overline{Q_F}$.

3. RESULTS AND DISCUSSION

3.1. Heat storage fluxes

Figure 3 shows the ESTM ensemble local-scale heat storage fluxes by layer for a summertime period (19 July–29 August 2002). Early in the day, ΔQ_S is driven by the storage in the roof layer; however, this layer is relatively thin, so ΔQ_S peaks before noon. Storage in external walls lags the roof peak by about 2 to 3 h. The external walls store almost as much heat as the roof owing to their larger mass, despite smaller diurnal temperature variation. The internal mass of the building element (iBLD, Figure 2) has the largest storage capacity, but it contributes little to diurnal changes in ΔQ_S since the temperature changes relatively slowly. Storage in the road layer is similar in phase to the walls and 80% of wall peak storage. Comparison of road storage with the Q_G measurement near the building shows differences in phase due to shading of the soil above the sensor; but, on average, these differences are within 10 W m^{-2}. Storage in the air column (air, Figure 1) is small but non-negligible. It is phase shifted to peak in the morning when air temperature is increasing most rapidly. Air temperature changes are more important on time scales shorter than a few hours than on a diurnally weighted basis.

Comparison with the other models shows only slight differences in phase and amplitude over the diurnal cycle (Figure 3). For this period, the daytime, $Q^* > 0$, ESTM heat storage flux for Łódź-Lipowa (70 W m^{-2}, 27% of Q^*) was greater than that of TEB (66 W m^{-2}, 25%) and slightly less than OHM (73 W m^{-2}, 27%). All estimates give positive mean ΔQ_S over this late summertime period. Both TEB and OHM put more

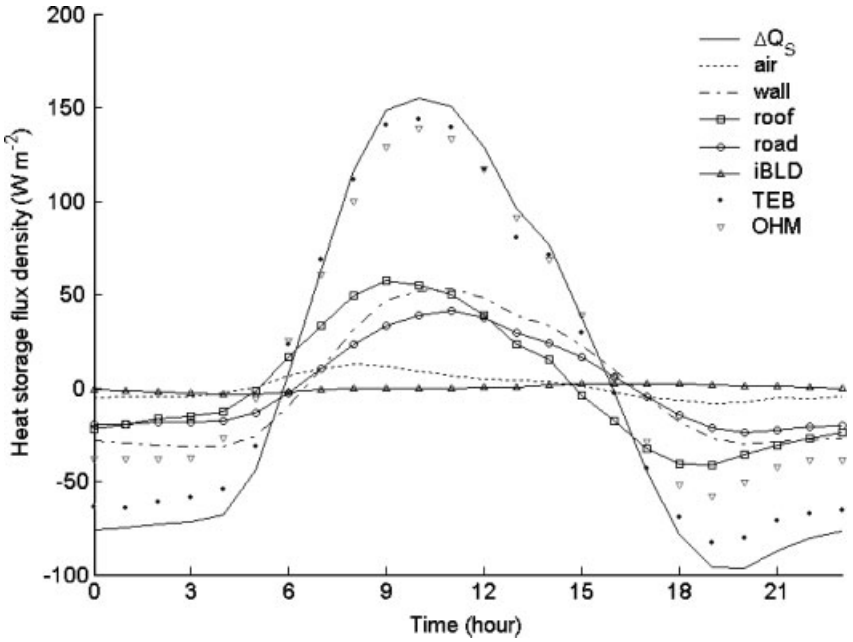

Figure 3. Modelled diurnal hourly heat storage fluxes over the period 19 July–29 August 2002. Shown are the total heat storage flux ΔQ_S, and that in the model elements: air column, mean wall, roof, road and soil, and the internal building mass (iBLD). Also shown are the estimates from TEB and OHM

energy into storage, 4.5 and 17 W m^{-2}, respectively, than did ESTM (0.5 W m^{-2}). The TEB scheme has also been used to model ΔQ_S for downtown Mexico City, a light industrial district of Vancouver, Canada (Masson *et al.*, 2002) and the city core of Marseille (Lemonsu *et al.*, 2004). The daytime estimate here is less than that for the more densely built sites of Mexico City in December (140 W m^{-2}, 54%) and Marseille in June; and it is slightly greater than the Vancouver site (70–76 W m^{-2}, 23%) over days 223–236 (Masson *et al.*, 2002; Lemonsu *et al.*, 2004). The diurnal course of ΔQ_S modelled for Łódź is more similar to the Vancouver than the Mexico City site. The Łódź–Lipowa site falls somewhere between the two sites in terms of heat storage characteristics, although the building volume area fraction (building fraction × building height) is only slightly greater than Vancouver (3.1 versus 3.0).

Since the storage term in TEB is equivalent to the heat conduction through the building elements, it was not directly compared with ESTM over the period (1 October–31 March) when a fixed inside building temperature (19 °C) was specified for TEB. The TEB results for the winter period show consistent outward conduction due to internal building heating, and temporal changes similar to ESTM.

Over the course of a year ΔQ_S is necessarily close to zero, −0.01 W m^{-2} and −0.04 W m^{-2} in 2001 and 2002 respectively. For the same period, the measured Q_G was −0.68 W m^{-2}. Over a single month, ΔQ_S ranges from −8 to +6 W m^{-2} (Figure 4). These values suggest that, for areas of a similar structure and meteorological forcings to Łódź, over monthly and longer time frames Q_F can be estimated from the measured energy balance residual, and the error resulting from neglecting changes in heat storage should be within ±10 W m^{-2}. The largest component on a monthly basis is typically the road and soil element. Because internal building temperature was not well regulated, storage changes in the internal mass can also be large. However, the noted spatial bias in the internal air temperature measurement may exaggerate this slightly. Despite the amount of above-ground mass, the monthly ESTM values are similar to values measured for $Q_G (R^2 = 0.68)$, suggesting that soil heat flux could be a reasonable approximation of the longer term storage changes. This result is sensitive to the road parameters, and, as building density and the amount of built surface increase, these patterns will likely show greater divergence. One consistent difference was

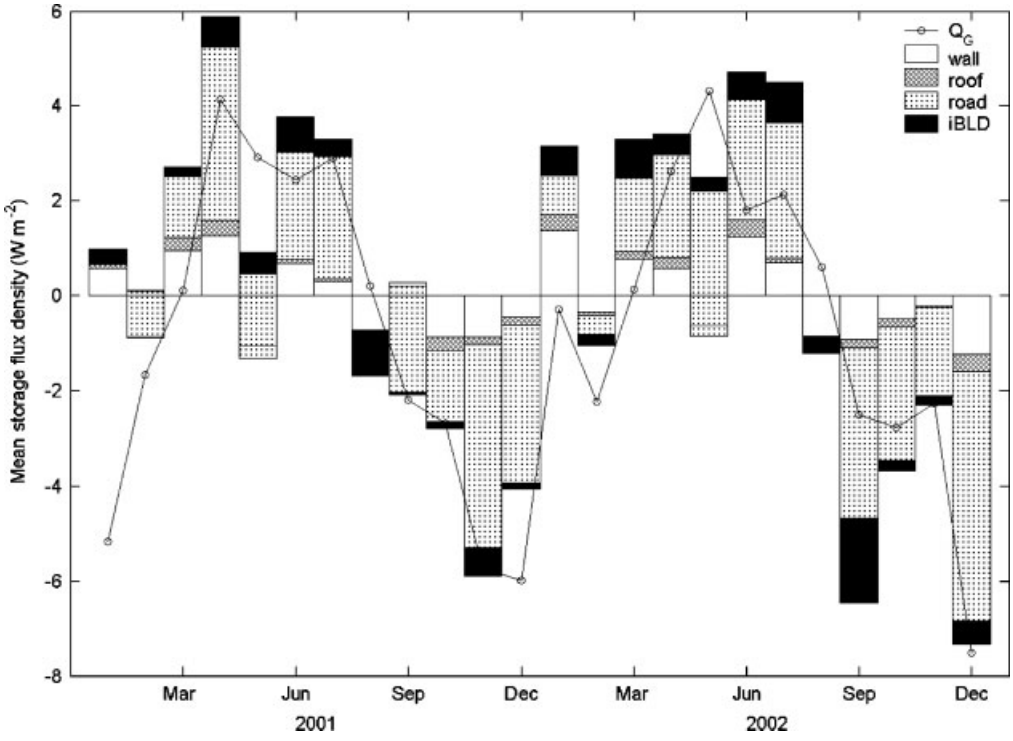

Figure 4. Monthly ΔQ_S by component and soil heat flux measurement Q_G for comparison

noted. From January to March of both years, Q_G was more negative than the modelled storage and showed an average release from storage 25 times greater than the model over the 2 years. This may have been due to soil water freezing above the heat flux plate but not below. Thus, more heat was conducted upward through the plate than in the surrounding soil.

3.2. Anthropogenic heat flux

Offerle *et al*. (in press) suggested that Q_F is a large component of the energy balance of Łódź in winter, but did not quantify the term. Kłysik's (1996) study of anthropogenic heating in Łódź, using monthly energy consumption data from the mid-1980s, suggests that Q_F probably exceeds Q^* for Łódź in much of the winter. For this area of Łódź, internal building heating is normally supplied by a central distribution system from October to April (Kłysik, 1996); otherwise, the Q_F sources are limited to human and vehicular traffic.

Although hourly determined values for Q_F are variable, since they incorporate all errors in the energy balance, the results are generally as expected. Mean Q_F is larger in winter than in summer and shows an inverse relationship with air temperature (Figure 5). During the October–March period the estimated Q_F increases by 2.7 ± 0.5 W m^{-2} per 1 °C decrease in temperature. The peak correlation ($r = 0.38$) occurs at a lag of between 6 and 8 h between temperature and Q_F. From June to August the monthly values are unrealistically negative (Figure 5), which indicates a lack of energy balance closure. Although this may be partially attributable to phase and amplitude errors in ΔQ_S, the longer term lack of closure is more likely due to consistent underestimation of the turbulent fluxes, overestimation of net radiation, or unaccounted sinks within system.

On a diurnal basis, the patterns of Q_F, shown in Figure 6 for summer and for October–March when space heating is available, do not coincide with what is expected. In summer, Q_F would be expected to peak during the day, possibly coinciding with increases in traffic. Such peaks are evident around expected peak traffic times (8 h and 17 h), and zero or slightly negative values at midday. Similar but smaller peaks are observed in the winter period when conduction through walls and mixing of heated building air should retard the

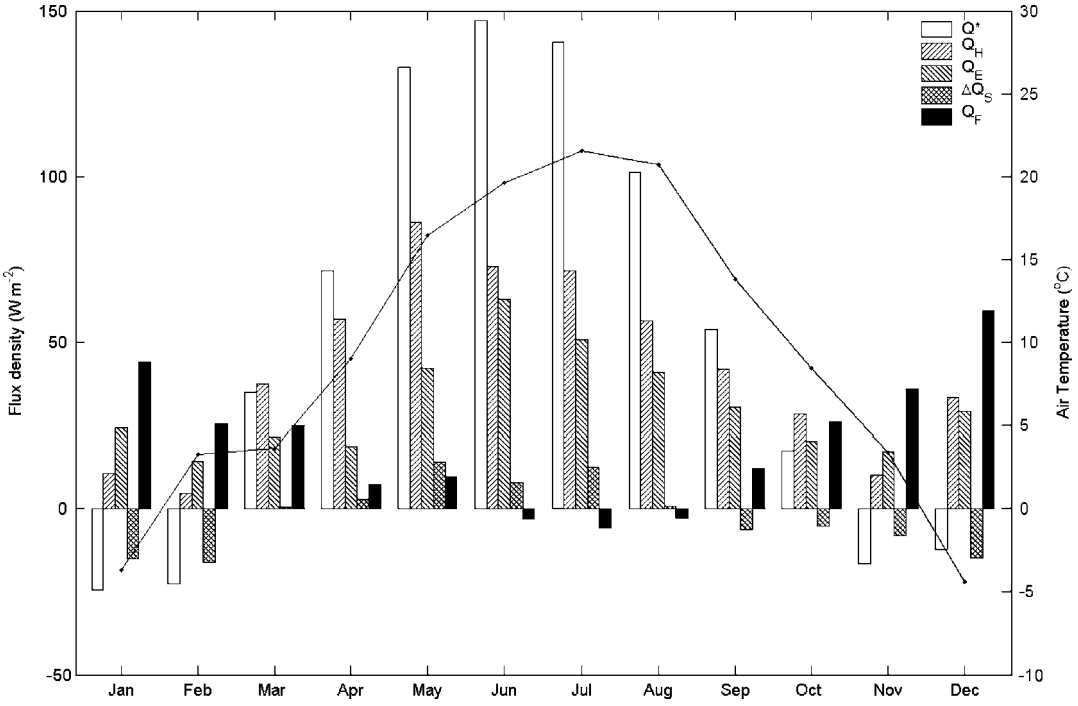

Figure 5. Monthly mean energy balance components and air temperature (line) for 2001–02. Values determined using periods when all components were valid

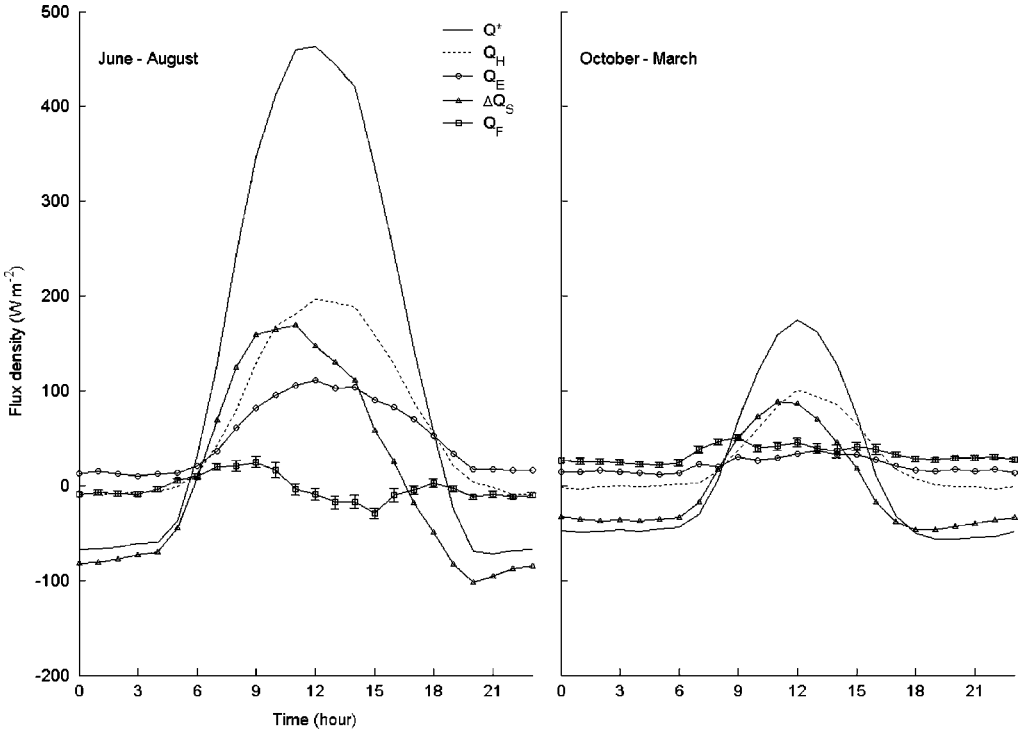

Figure 6. Diurnal pattern of energy balance fluxes for 2001–02. Error bars for Q_F are ±1 standard deviation

response of Q_F to diurnal forcings. However, the relative uncertainty in both the measured and estimated terms cautions us against inferring a direct relation with diurnal anthropogenic forcing.

3.3. Energy balance closure

Over natural surfaces, closure of the energy balance is sometimes used to evaluate the certainty of EC measurements (Wilson *et al.*, 2002). The linear regression of $Q_H + Q_E$ on $Q^* - \Delta Q_S$ (since hourly Q_F is unknown) yielded the results shown in Figure 7 for the summer and October–March periods. These estimates of closure (~0.95 for both periods) are in the upper half of the range reported by Wilson *et al.* (2002), although R^2 values are slightly lower. Available energy calculated with the TEB ΔQ_S yielded a lower slope (~0.88) for both periods and nearly identical R^2 values. The lower R^2 values may be attributable to the errors in ΔQ_S noted above, to the variable contribution of Q_F, particularly in winter, and unaccounted terms in the energy balance. Since the slope is less than one, the estimate of Q_F is negatively biased, assuming no other systematic biases in the data.

Over vegetated surfaces, the intercept of the regression is not attributed to a physical cause (Wilson *et al.*, 2002; Oliphant *et al.*, 2004). Here, as noted, if we assume that the anthropogenic fluxes represent a relatively constant addition to the available energy, then the intercept can be interpreted as $Q_F + \varepsilon$. In summer this assumption is likely better met, because Q_F is less affected by environmental conditions and the intercept for the regressions is near zero, 1.8 W m^{-2}; over October–March it is 33 W m^{-2} (Figure 7). The values are similar to the residual calculated Q_F of −3.5 W m^{-2} and 32 W m^{-2}. The values calculated from Kłysik (1996) for these periods are 21 W m^{-2} and 55 W m^{-2} respectively. During some of the colder periods, measurements were prevented due to the accumulation of ice on the sensors. Some of the times of peak wintertime heating are not included in this estimate, and values reported here should, therefore, be lower than those presented by Kłysik (1996).

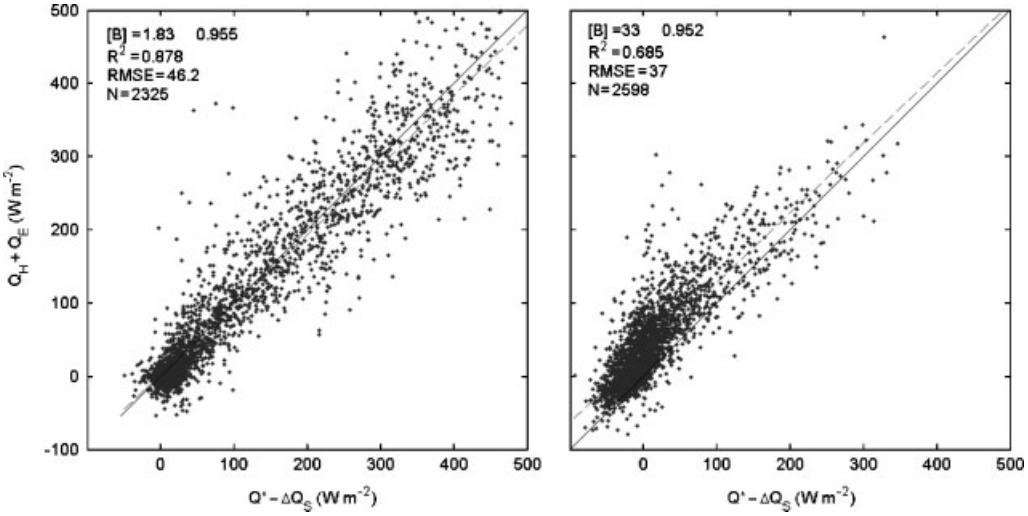

Figure 7. Regression of turbulent flux sum on available energy for summer (June–August) and winter (October–March). Statistics in the first row are the intercept and slope respectively

3.4. Factors related to the energy imbalance

The scatter for both summer and winter periods and the variable anthropogenic heat source caution against making inferences about the direct causes for lack of energy balance closure, but here we examine the relationships with possible contributing factors.

Wilson *et al*. (2002) note that their, and prior, studies indicate that restricting the data to higher values of u^* improves energy balance closure; this was also noted to be more of a factor at night (Oliphant *et al*., 2004). The energy balance ratio shows little or no correlation with either wind speed or friction velocity u^* during the daytime ($Q^* > 0$), although variability decreases with increasing u^* (Figure 8). A dense forest canopy may prevent mixing between above- and below-canopy layers when turbulence is weak or episodic. Over an urban surface, of the obstacle spacing of Łódź, eddies are freer to penetrate into the canyons and the bluff obstacles enhance mixing within the canyons. Hence, it appears that even under weak turbulence when the EC measurements have greater uncertainty, they are not significantly biased in unstable conditions. At night, with more neutral to stable conditions, the weaker turbulent mixing appears to be a factor, although with greater scatter due to small values in the denominator (Figure 8). For the night-time measurements the energy balance ratio does not approach one until u^* increases above 0.4 m s^{-1}. This is slightly greater than the 0.3 m s^{-1} value given for forests (Oliphant *et al*., 2004).

Of the other factors cited by Wilson *et al*. (2002) as possibly contributing to lack of closure, specifically considering the nature of urban climates, it seems likely that advection could account for some of the imbalance. Horizontal advection should be manifest in a directional dependence of the fluxes, increasing with positive horizontal gradients of the scalars in the direction of the mean wind (Ching *et al*., 1983). The measurement site is located to the east of the peak urban–rural temperature difference shown by Kłysik and Fortuniak (1999). Therefore, we would expect enhanced (diminished) turbulent sensible heat fluxes with westerly (easterly) flow when an urban heat island exists. Since this is nearly opposite to the effect of expected Q_F contributions (the impact of the local source area characteristics), it may be harder to detect. Figure 9 shows the dependence of the energy balance ratio on wind direction. During the day, when urban–rural temperature differences are not so pronounced, there is little directional dependency, except for the previously excluded wind directions where source areas were more predominantly vegetated. In these sectors (210–270°), source-area characteristics are sufficiently different that the ΔQ_S value should change as well. At night, the ratio is in agreement with the expected advective influence, but the restriction to u^*, to reduce the dependence on turbulence, leaves few observations from some wind sectors (Figure 9).

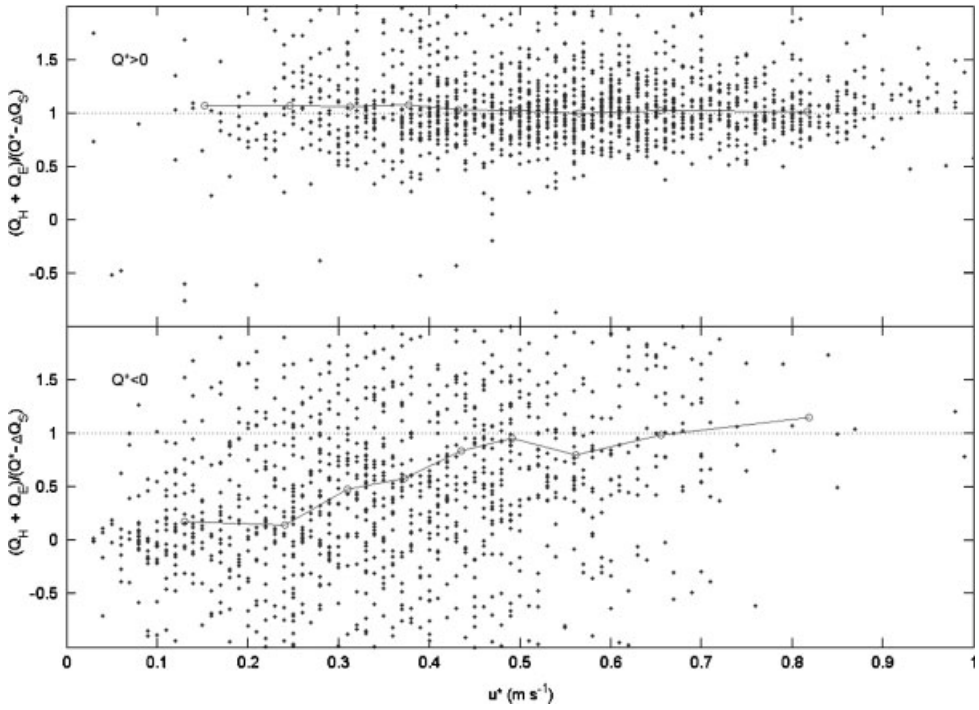

Figure 8. Energy balance ratio as a function of friction velocity u^* for June–September for daytime ($Q^* > 0$) and night-time ($Q^* < 0$). The line shows the ratio determined over equally distributed bins in u^*

4. CONCLUSIONS

Over complex surfaces, accurately determining heat storage based on turbulent flux measurements is difficult due to measurement uncertainty, longer time-scale heat storage changes, and variation in source-area composition. Over urban surfaces, this is complicated by the addition of a sometimes large anthropogenic heat source. Using a small number of representative surface temperature measurements, it is possible to estimate heat storage fluxes on the relevant time scales. This estimate of ΔQ_S independent of the turbulent flux measurements indicates that storage fluxes play an important role controlling the exchange of energy between the urban surface and the atmosphere on the scale of hours to days. Even over longer periods, ΔQ_S can contribute an important fraction of the available energy, but it is generally dominated by the other source terms over scales longer than a day. Because of the importance of local-scale ΔQ_S, future urban energy balance observations should try to incorporate similar, and preferably more complete, measurements and model estimates than those presented here.

Despite the limitations of the ΔQ_S estimate, it allowed for testing energy balance closure over shorter intervals when ΔQ_S cannot be assumed to be equal to zero, as well as when the measurements form an incomplete time series. Here, there was a high degree of energy balance closure throughout the year. Although closure was only slightly lower in winter, there was less agreement between available energy and the turbulent fluxes. This was attributed to random errors in ΔQ_S and greater variation in Q_F. It was noted that turbulent fluxes appear to be underestimated, which could not be assigned to a single causal factor. Without more complete measurements to evaluate ΔQ_S it is difficult to assess precisely the causes of the underestimation.

The energy balance residual was assumed to be representative of the anthropogenic flux contribution with added uncertainty due to errors in measurement and unaccounted terms in the energy balance. Although this led to physically unrealistic values over intervals shorter than a day, as well as during the summer period, over the year it was consistent with the pattern of anthropogenic heat input. For summer, this value was slightly negative (-3 W m^{-2}), and for October–March was 32 W m^{-2} and showed an inverse relationship with air

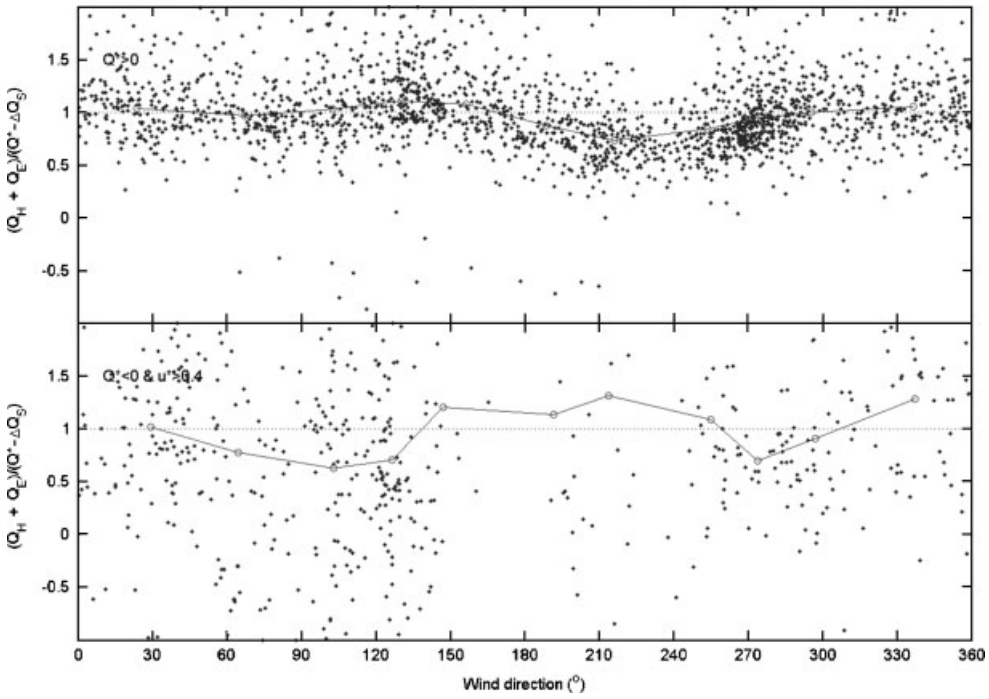

Figure 9. Energy balance ratio by wind direction. Division is same as Figure 8, except night-time values are restricted to $u^* > 0.4$ m s^{-1}. Wind directions previously excluded from analysis are shown here for completeness

temperature. The value computed for the summer is likely below any measurable anthropogenic contribution by this approach. In winter, when the anthropogenic contribution is considerably larger, it produces a more reasonable estimate, but still negatively biased judging from the lack of closure.

ACKNOWLEDGEMENTS

Funding for this research was provided by the NSF 0095284, NSF 0221105, NATO 977460 and Polish Academy of Sciences. Dr Catherine Souch provided instrumentation to support this project. Professor K. Kłysik, Dr Joanna Wibig, and the graduate students within their department, provided invaluable support to this project. Dr Valery Masson, Meteo-France, provided access to and assistance with TEB.

REFERENCES

Arnfield AJ, Grimmond CSB. 1998. An urban canyon energy budget model and its application to urban storage heat flux modelling. *Energy and Buildings* **27**: 61–68.

ASHRAE. 1981. *ASHRAE Handbook: 1981 Fundamentals*. American Society of Heating, Refrigerating and Air-Conditioning Engineers: Atlanta.

Awbi HB, Hatton A. 1999. Natural convection from heated room surfaces. *Energy and Buildings* **30**: 233–244.

Best M, Clark PA. 2002. The influence of vegetation on the urban climate. In *Fourth Symposium on the Urban Environment*, 20–24 May 2002, Norfolk, VA. American Meteorological Society: 88–89.

Ching JKS, Clarke JF, Godowitch JM. 1983. Modulation of heat flux by different scales of advection in an urban environment. *Boundary-Layer Meteorology* **25**: 171–191.

Ellefsen R. 1990. Mapping and measuring buildings in the canopy boundary layer in ten US cities. *Energy and Buildings* **15–16**: 1025–1049.

Grimmond CSB. 1992. The suburban energy balance: methodological considerations and results for a mid-latitude West Coast city under winter and spring conditions. *International Journal of Climatology* **12**: 481–497.

Grimmond CSB, Oke TR. 1999. Heat storage in urban areas: observations and evaluation of a simple model. *Journal of Applied Meteorology* **38**: 922–940.

Grimmond CSB, Oke TR. 2002. Turbulent heat fluxes in urban areas: observations and a local-scale urban meteorological parameterization scheme (LUMPS). *Journal of Applied Meteorology* **41**: 792–810.

Grimmond CSB, Cleugh HA, Oke TR. 1991. An objective urban heat storage model and its comparison with other schemes. *Atmospheric Environment B* **25**: 311–326.
Goulden ML, Munger JW, Fan FM, Daube BC, Wofsy SC. 1996. Measurements of carbon sequestration by long-term eddy covariance: methods and a critical evaluation of accuracy. *Global Change Biology* **2**: 169–182.
Ichinose T, Shimodozono K, Hanaki K. 1999. Impact of anthropogenic heat on urban climate in Tokyo. *Atmospheric Environment* **33**: 3897–3909.
Kłysik K. 1996. Spatial and seasonal distribution of anthropogenic heat emissions in Łódź, Poland. *Atmospheric Environment* **30**: 3397–3404.
Kłysik K, Fortuniak K. 1999. Temporal and spatial characteristics of the urban heat island of Łódz, Poland. *Atmospheric Environment* **33**: 3885–3895.
Kusaka H, Kondo H, Kikegawa Y, Kimura F. 2001. A simple single-layer urban canopy model for atmospheric models: comparison with multi-layer and slab models. *Boundary-Layer Meteorology* **101**: 329–358.
Lemonsu A, Grimmond CSB, Masson V. 2004. Modelling the surface energy balance of an old Mediterranean city core. *Journal of Applied Meteorology* **43**: 312–327.
Masson V. 2000. A physically-based scheme for the urban energy balance in atmospheric models. *Boundary-Layer Meteorology* **94**: 357–397.
Masson V, Grimmond CSB, Oke TR. 2002. Evaluation of the Town Energy Balance (TEB) scheme with direct measurements from dry districts in two cities. *Journal of Applied Meteorology* **41**: 1011–1026.
Meyn SK. 2000. Heat fluxes through roofs and their relevance to estimates of urban heat storage. MS thesis, Department of Geography, University of British Columbia, Vancouver, BC, Canada. (Available from T. Oke at toke@geog.ubc.ca.).
Moncrieff JB, Malhi Y, Leuning R. 1996. The propagation of errors in long-term measurements of land–atmosphere fluxes of carbon and water. *Global Change Biology* **2**: 231–240.
Nemitz E, Hargreaves KJ, McDonald AG, Dorsey JR, Fowler D. 2002. Micrometeorological measurements of the urban heat budget and CO_2 emissions on a city scale. *Environmental Science and Technology* **36**: 3139–3146.
Nunez M, Oke TR. 1977. The energy balance of an urban canyon. *Journal of Applied Meteorology* **16**: 11–19.
Offerle B, Grimmond CSB, Oke TR. 2003. Parameterization of net all-wave radiation for urban areas. *Journal of Applied Meteorology* **42**: 1157–1173.
Offerle B, Grimmond CSB, Fortuniak K, Kłysik K, Oke TR. In press. Temporal variations in heat fluxes over a central European city centre. *Theoretical and Applied Climatology*.
Oke TR. 1987. *Boundary Layer Climates*. Routledge: London.
Oke TR. 1988. The urban energy balance. *Progress in Physical Geography* **12**: 471–508.
Oke TR. 1997. Urban environments. In *The Surface Climates of Canada*, Bailey WG, Oke TR, Rouse WR (eds). McGill-Queen's University Press: Montréal; 303–327.
Oke TR. 2004. Initial guidance to obtain representative meteorological observations at urban sites. WMO Instruments and Observing Methods Report No. 81, WMO/TD 1250, 51 pp.
Oliphant A, Grimmond CSB, Zutter H, Schmid HP, Su H-B, Scott SL, Offerle B, Randolph JC, Ehman J. 2004. Heat storage and energy balance fluxes for a temperate deciduous forest. *Agricultural and Forest Meteorology* **126**: 185–201.
Roth M, Oke TR. 1993. Turbulent transfer relationships over an urban surface I. Spectral characteristics. *Quarterly Journal of the Royal Meteorological Society* **119**: 1071–1104.
Rotach MW. 1995. Profiles of turbulence statistics in and above an urban street canyon. *Atmospheric Environment* **29**: 1473–1486.
Rotach MW. 1999. On the influence of the urban roughness sublayer on turbulence and dispersion. *Atmospheric Environment* **33**: 4001–4008.
Sailor DJ, Lu L. 2004. A top-down methodology for developing diurnal and seasonal anthropogenic heating profiles for urban areas. *Atmospheric Environment* **38**: 2737–2748.
Schmid HP. 1997. Experimental design for flux measurements: matching scales of observations and fluxes. *Agricultural and Forest Meteorology* **87**: 179–200.
Schmid HP, Cleugh HA, Grimmond CSB, Oke TR. 1991. Spatial variability of energy fluxes in suburban terrain. *Boundary-Layer Meteorology* **54**: 249–276.
Sellers WD. 1966. *Physical Climatology*. University of Chicago Press: Chicago.
Spronken-Smith RA. 2002. Comparison of summer- and winter-time suburban energy fluxes in Christchurch, New Zealand. *International Journal of Climatology* **22**: 979–992.
Su HB, Schmid HP, Grimmond CSB, Vogel CS, Oliphant AJ. 2004. Spectral characteristics and correction of long-term eddy-covariance measurements over two mixed hardwood forests in non-flat terrain. *Boundary-Layer Meteorology* **110**: 213–253.
Taha H. 1999. Modifying a mesoscale meteorological model to better incorporate urban heat storage: a bulk-parameterization approach. *Journal of Applied Meteorology* **38**: 466–473.
Theurer W. 1999. Typical building arrangements for urban air pollution modelling. *Atmospheric Environment* **33**: 4057–4066.
Vickers D, Mahrt L. 1997. Quality control and flux sampling problems for tower and aircraft data. *Journal of Atmospheric and Oceanic Technology* **14**: 512–526.
Wilson K, Goldstein A, Falge E, Aubinet M, Baldocchi D, Berbigier P, Bernhofer C, Ceulemans R, Dolman H, Field C, Grelle A, Ibrom A, Law BE, Kowalski A, Meyers T, Moncrieff J, Monson R, Oechel W, Tenhunen J, Valentini R, Verma S. 2002. Energy balance closure at FLUXNET sites. *Agricultural and Forest Meteorology* **113**: 223–243.

